

Fluoro Complexes of Permethyltantallocene, $\text{Cp}^*_2\text{TaF}_3$ and $[\text{Cp}^*_2\text{TaF}_2][\text{BF}_4]$: Facile Formation of a Tetrafluoroborate Complex via Corrosion of Borosilicate Glass

Jun Ho Shin and Gerard Parkin*

Department of Chemistry, Columbia University, New York, New York 10027

Received June 29, 1998

The trihydride complex $\text{Cp}^*_2\text{TaH}_3$ is a convenient precursor to a series of halide derivatives, which include unusual examples of organometallic fluoride complexes. Most interestingly, reaction of $\text{Cp}^*_2\text{TaH}_3$ with $(\text{C}_5\text{H}_5\text{N})(\text{HF})_x$ affords the trifluoride complex $\text{Cp}^*_2\text{TaF}_3$ when carried out in a plastic vessel, but the tetrafluoroborate complex $[\text{Cp}^*_2\text{TaF}_2][\text{BF}_4]$ when performed in a borosilicate glass vessel. In contrast, reaction of $\text{Cp}^*_2\text{TaH}_3$ with $[\text{Et}_3\text{N}(\text{HF})_3]$ results in cleavage of one of the pentamethylcyclopentadienyl ligands to yield the half-sandwich complex $[\text{Et}_3\text{NH}][\text{Cp}^*\text{TaF}_5]$. $\text{Cp}^*_2\text{TaF}_3$ and $[\text{Cp}^*_2\text{TaF}_2][\text{BF}_4]$ may be readily interconverted. Thus, treatment of $\text{Cp}^*_2\text{TaF}_3$ with either $\text{Et}_2\text{O}\cdot\text{BF}_3$ or LiBF_4 yields $[\text{Cp}^*_2\text{TaF}_2][\text{BF}_4]$, while reaction of the latter complex with excess NaF regenerates $\text{Cp}^*_2\text{TaF}_3$. Furthermore, $\text{Cp}^*_2\text{TaF}_3$ is converted to the cyano fluoride complex $\text{Cp}^*_2\text{Ta}(\text{CN})_2\text{F}$ upon reaction with excess Me_3SiCN . Sequential replacement of the hydride ligands of $\text{Cp}^*_2\text{TaH}_3$ is observed in the reaction with MeI to give $\text{Cp}^*_2\text{TaH}_2\text{I}$ and $\text{Cp}^*_2\text{TaHI}_2$; likewise, the reactions of $\text{Cp}^*_2\text{TaH}_3$ with either HCl , CHCl_3 , or CCl_4 give $\text{Cp}^*_2\text{TaH}_2\text{Cl}$ and $\text{Cp}^*_2\text{TaHCl}_2$. The molecular structures of $[\text{Cp}^*_2\text{TaF}_2][\text{BF}_4]$, $[\text{Et}_3\text{NH}][\text{Cp}^*\text{TaF}_5]$, and $\text{Cp}^*_2\text{TaHCl}_2$ have been determined by X-ray diffraction.

Introduction

Even though it is recognized that the chemistry of metal–fluoro complexes is frequently atypical from that of other halide derivatives,¹ organometallic fluoro complexes have received substantially less attention than their chloro, bromo, and iodo counterparts.² For example, with respect to tantalum, organometallic fluoro complexes are presently restricted to $(\text{Bu}^i\text{CH}_2)_3\text{TaF}_3$ and half-sandwich cyclopentadienyl derivatives.^{2,4,5} One of the principal factors responsible for the paucity of organometallic fluoro complexes is the lack of convenient synthetic methods.² Therefore, in this paper, we describe simple procedures for the syntheses of fluoro complexes of permethyltantallocene, namely, $\text{Cp}^*_2\text{TaF}_3$

(1) See, for example: Caulton, K. G. *New J. Chem.* **1994**, *18*, 25–41.

(2) (a) Murphy, E. F.; Murugavel, R.; Roesky, H. W. *Chem. Rev.* **1997**, *97*, 3425–3468. (b) Doherty, N. M.; Hoffman, N. W. *Chem. Rev.* **1991**, *91*, 553–573. (c) Walawalker, M. G.; Murugavel, R.; Roesky, H. W. *Eur. J. Solid State Inorg. Chem.* **1996**, *33*, 943–955.

(3) Schrock, R. R.; Fellman, J. D. *J. Am. Chem. Soc.* **1978**, *100*, 3359–3370.

(4) For example: Cp^*TaF_4 , $[\text{Cp}^*\text{TaF}_3(\mu\text{-F})_2\cdot 2(\text{AsF}_6)]$, $\text{Cp}^*\text{TaF}_4\cdot(\text{HN}=\text{PPh}_3)$, and $\text{Cp}^*\text{TaF}_3[\text{OC}(\text{R})\text{CHC}(\text{R})\text{O}]$. (a) Roesky, H. W.; Schruppf, F.; Noltemeyer, M. *J. Chem. Soc., Dalton Trans.* **1990**, 713–714. (b) Roesky, H. W.; Schruppf, F.; Noltemeyer, M. *Z. Naturforsch.* **1989**, *44b*, 1369–1372. (c) Schruppf, F.; Roesky, H. W.; Noltemeyer, M. *Z. Naturforsch.* **1990**, *45b*, 1600–1602. (d) Schruppf, F.; Roesky, H. W.; Subrahmanyam, T.; Noltemeyer, M. *Z. Anorg. Allg. Chem.* **1990**, *538*, 124–132.

(5) For other examples of tantalum fluoride complexes, see: (a) Dewan, J. C.; Edwards, A. J.; Calves, J. Y.; Guerschais, J. E. *J. Chem. Soc., Dalton Trans.* **1977**, 981–983. (b) Dewan, J. C.; Edwards, A. J.; Calves, J. Y.; Guerschais, J. E. *J. Chem. Soc., Dalton Trans.* **1977**, 978–980. (c) McLoughlin, M. A.; Keder, N. L.; Kaska, W. C. *Acta Crystallogr.* **1992**, *C48*, 1098–1099.

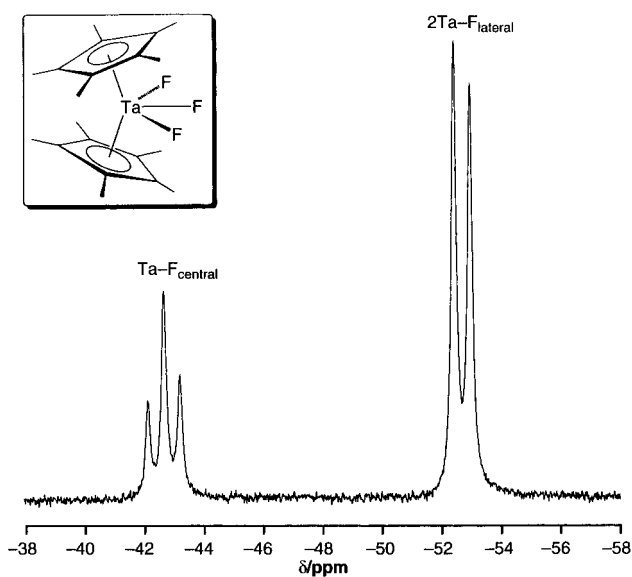


Figure 1. ^{19}F NMR spectrum of $\text{Cp}^*_2\text{TaF}_3$ in CDCl_3 .

and $[\text{Cp}^*_2\text{TaF}_2][\text{BF}_4]$ ($\text{Cp}^* = \text{C}_5\text{Me}_5$). Interestingly, the $[\text{BF}_4]^-$ counterion in the latter complex may be derived via corrosion of the borosilicate glass reaction vessel.

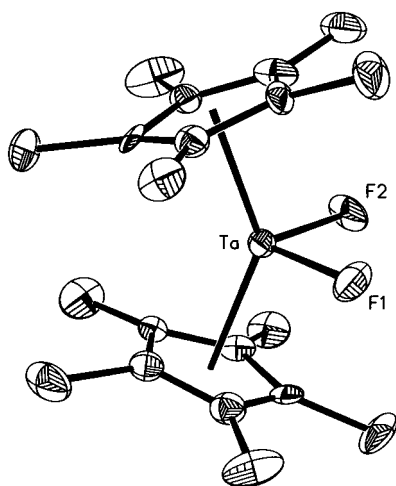
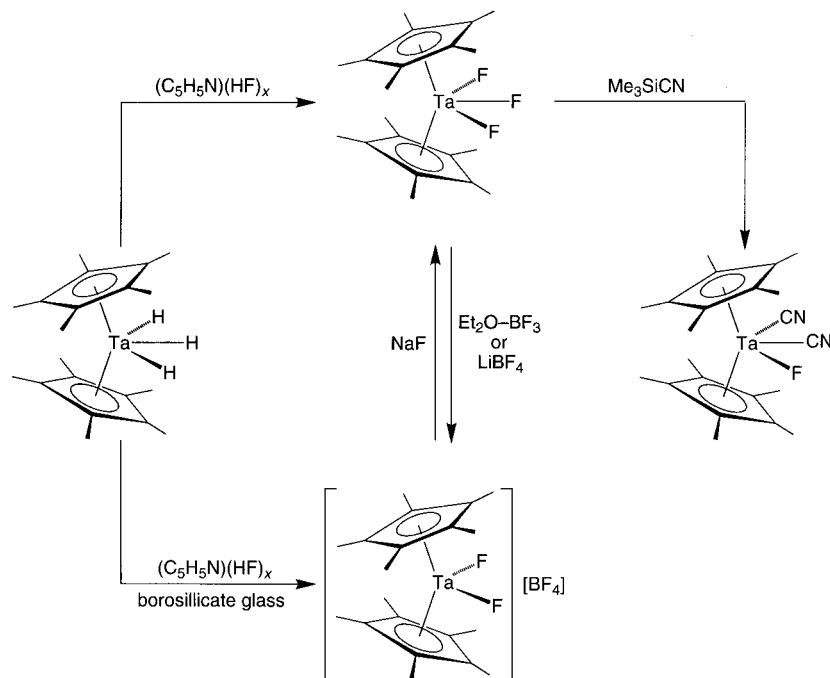
Results and Discussion

Bercaw has demonstrated that the permethyltantallocene moiety is capable of supporting a diverse array of unusual ligand combinations, as illustrated by the methylene–hydride and oxo–hydride complexes,

Table 1. ^{19}F NMR Spectroscopic Data for Pentamethylcyclopentadienyl Tantalum Fluoride Complexes

	δ (ppm)	$^2J_{\text{F-F}}$ (Hz)	ref
$\text{Cp}^*_2\text{TaF}_3$	-42.6 (t), -52.6 (d)	153	this work
$[\text{Cp}^*_2\text{TaF}_2][\text{BF}_4]$	21.2 (s) ^a		this work
$\text{Cp}^*_2\text{TaF}(\text{CN})_2$	-194.1 (s)		this work
$[\text{Et}_3\text{NH}][\text{Cp}^*\text{TaF}_5]$	12.9 (d), -16.2 (quin) ^b	90	this work
$\text{Cp}^*\text{TaF}_3[(\text{Me}_3\text{SiN})_2\text{C}(p\text{-C}_6\text{H}_5)]$	6.4 (t), 71.7 (d)	91	<i>d</i>
$\text{Cp}^*\text{TaF}_3[(\text{Me}_3\text{SiN})_2\text{C}(p\text{-C}_6\text{H}_4\text{CF}_3)]$	8.6 (t), 73.8 (d) ^c	90	<i>d</i>
$\text{Cp}^*\text{TaF}_3[(\text{Me}_3\text{SiN})_2\text{C}(p\text{-C}_6\text{H}_4\text{NMe}_2)]$	8.0 (t), 71.3 (d)	94	<i>d</i>
$\text{Cp}^*\text{TaF}_3[(\text{Me}_3\text{SiN})_2\text{C}(p\text{-C}_6\text{H}_4\text{CH}_3)]$	7.6 (t), 71.1 (d)	90	<i>d</i>
$\text{Cp}^*\text{TaF}_3[(\text{Me}_3\text{SiN})_2\text{C}(p\text{-C}_6\text{H}_4\text{CN})]$	13.5 (t), 75.0 (d)	90	<i>d</i>
$\text{Cp}^*\text{TaF}_3[(\text{Me}_3\text{SiN})_2\text{C}(p\text{-C}_6\text{H}_4\text{OMe})]$	7.2 (t), 70.8 (d)	91	<i>d</i>

^a $[\text{BF}_4]$ group is observed at -154.6 ppm. ^b Concentration of $[\text{Et}_3\text{NH}][\text{Cp}^*\text{TaF}_5]$ is 0.08 M. ^c CF_3 group is observed at -63.2 ppm. ^d Schrupf, F.; Roesky, H. W.; Subrahmanyam, T.; Noltemeyer, M. Z. *Anorg. Allg. Chem.* **1990**, 538, 124-132.

Scheme 1**Figure 2.** Molecular structure of $[\text{Cp}^*_2\text{TaF}_2][\text{BF}_4]$ (only cation is shown).

$\text{Cp}^*_2\text{Ta}(\text{CH}_2)\text{H}$ and $\text{Cp}^*_2\text{Ta}(\text{O})\text{H}$.⁶ As such, we considered that fluoro derivatives may also be accessible for

(6) (a) van Asselt, A.; Burger, B. J.; Gibson, V. C.; Bercaw, J. E. *J. Am. Chem. Soc.* **1986**, 108, 5347-5349. (b) Antonelli, D. M.; Schaefer, W. P.; Parkin, G.; Bercaw, J. E. *J. Organomet. Chem.* **1993**, 462, 213-220.

Table 2. Selected Bond Lengths (Å) and Angles (deg) for $[\text{Cp}^*_2\text{TaF}_2][\text{BF}_4]$

Ta-F(1)	1.925(12)	Ta-F(2)	1.874(12)
Ta-C(11)	2.436(19)	Ta-C(12)	2.442(20)
Ta-C(13)	2.432(17)	Ta-C(14)	2.412(18)
Ta-C(15)	2.438(15)	Ta-C(21)	2.417(20)
Ta-C(22)	2.385(18)	Ta-C(23)	2.417(18)
Ta-C(24)	2.443(17)	Ta-C(25)	2.421(19)
F(1)-Ta-F(2)	96.1(6)		

this system. Indeed, the tantalum(V) fluoride complex $\text{Cp}^*_2\text{TaF}_3$ is readily synthesized by treatment of the hydride derivative $\text{Cp}^*_2\text{TaH}_3$ with pyridinium poly(hydrogen fluoride), $[(\text{C}_5\text{H}_5\text{N})(\text{HF})_x]$,⁷ in a plastic reaction vessel. Decisive evidence that characterizes the product as the trifluoride $\text{Cp}^*_2\text{TaF}_3$ is provided by ^{19}F NMR spectroscopy. Specifically, the ^{19}F NMR spectrum consists of triplet and doublet resonances at δ -42.6 and -52.6 ppm ($^2J_{\text{F-F}} = 153$ Hz), assigned to the central and lateral fluorine ligands, respectively (Figure 1); as such, the form of the ^{19}F NMR spectrum is closely analogous to the ^1H NMR spectrum of its hydride counterpart, $\text{Cp}^*_2\text{TaH}_3$.⁸ The $^2J_{\text{F-F}}$ coupling constant of 153 Hz is substantially greater than the values in

(7) $x \approx 9$. See: Olah, G. A.; Welch, J. T.; Vankar, Y. D.; Nojima, M.; Kerekes, I.; Olah, J. A. *J. Org. Chem.* **1979**, 44, 3872-3881.

Scheme 2

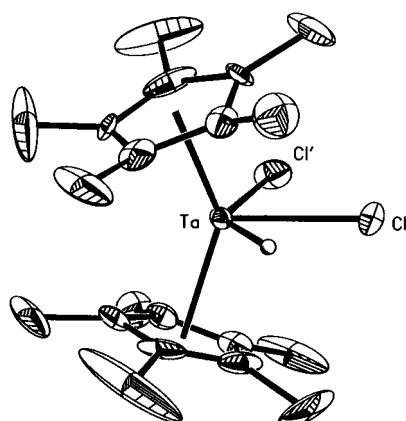
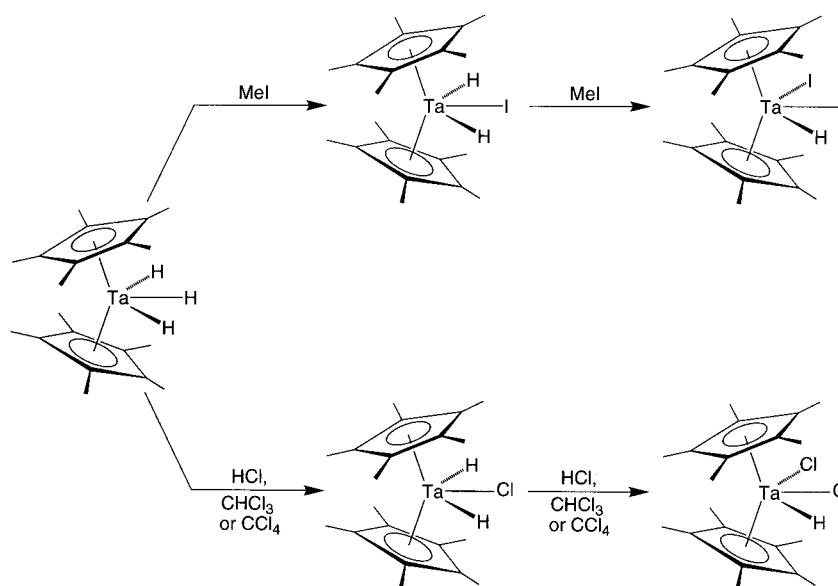


Figure 3. Molecular structure of $\text{Cp}^*_2\text{TaHCl}_2$ (the hydride ligand was not refined).

the majority of other pentamethylcyclopentadienyl tantalum fluoride complexes (Table 1).

The isolation of the Ta(V) fluoride complex $\text{Cp}^*_2\text{TaF}_3$ is of particular interest since tantalocene halide complexes are more commonly encountered as 17-electron Ta(IV) derivatives, $[\text{Cp}^R]_2\text{TaX}_2$, rather than as 18-electron Ta(V) complexes, $[\text{Cp}^R]_2\text{TaX}_3$.^{9–11} Specifically, a discussion of organometallic fluoro complexes of the group 5 elements in a recent review states, “the presence

(8) The hydride ligands of $\text{Cp}^*_2\text{TaH}_3$ are identified by triplet and doublet resonances at 1.11 and -0.91 ppm, respectively, with $^2J_{\text{H-H}} = 13$ Hz. See: Gibson, V. C.; Bercau, J. E.; Bruton, W. J., Jr.; Santer, R. D. *Organometallics* **1986**, *5*, 976–979.

(9) (a) Labinger, J. A. In *Comprehensive Organometallic Chemistry*; Wilkinson, G., Stone, F. G. A., Abel, E. W., Eds.; Pergamon: Oxford, U.K., 1982; Vol. 3, Chapter 25, p 766. (b) Wigley, D. E.; Gray, S. D. In *Comprehensive Organometallic Chemistry II*; Abel, E. W., Stone, F. G. A., Wilkinson, G., Eds.; Pergamon: Oxford, U.K., 1995; Vol. 5, Chapter 2, p 121.

(10) It should, nevertheless, be noted that chloro, bromo, and iodo derivatives of the class Cp^R_2MX_3 ($M = \text{Nb, Ta}$; $X = \text{Cl, Br, I}$) have been described in the literature, although their structures have not been authenticated by X-ray diffraction. (a) Wilkinson, G.; Birmingham, J. M. *J. Am. Chem. Soc.* **1954**, *76*, 4281–4284. (b) Chang, B.-H.; Tung, H.-S.; Brubaker, C. H., Jr. *Inorg. Chim. Acta* **1981**, *51*, 143–148. (c) Antiñolo, A.; Fajardo, M.; Otero, A.; Royo, P. *J. Organomet. Chem.* **1984**, *265*, 35–43. (d) Urbanos, F. A.; Mena, M.; Royo, P.; Antiñolo, A. *J. Organomet. Chem.* **1984**, *276*, 185–192. (e) Castro, A.; Gómez, M.; Gómez-Sal, P.; Manzanero, A.; Royo, P. *J. Organomet. Chem.* **1996**, *518*, 37–46.

Table 3. Selected Bond Lengths (Å) and Angles (deg) for $\text{Cp}^*_2\text{TaHCl}_2$

Ta–Cl	2.499(14)	Ta–C(11)	2.46(2)
Ta–C(12)	2.42(2)	Ta–C(13)	2.47(2)
Ta–C(14)	2.43(2)	Ta–C(15)	2.45(3)
Cl–Ta–Cl'	76.8(6)		

of two cyclopentadienyl groups and three halide atoms would result in a severely crowded coordination sphere in high oxidation state metallocene fluorides and this type of compound has not been reported”.^{2a,10} In this regard, the synthesis of $\text{Cp}^*_2\text{TaF}_3$ represents a notable development for organometallic tantalum fluoride chemistry.

Providing a marked contrast to the formation of the trifluoride $\text{Cp}^*_2\text{TaF}_3$ upon treatment of $\text{Cp}^*_2\text{TaH}_3$ with $[(\text{C}_5\text{H}_5\text{N})(\text{HF})_x]_n$ in a plastic vessel, the corresponding reaction performed in a borosilicate glass vessel reproducibly yields the *tetrafluoroborate* complex $[\text{Cp}^*_2\text{TaF}_2][\text{BF}_4]$ (Scheme 1). The presence of the $[\text{BF}_4]^-$ counterion is presumably a consequence of corrosion of the borosilicate glass by $[(\text{C}_5\text{H}_5\text{N})(\text{HF})_x]_n$.^{12,13} Although the formation of complexes in which a tetrafluoroborate counterion is derived from glass is uncommon, it is, nevertheless, precedented. For example, the reaction of *cis*- $[\text{W}(\text{N}_2)_2(\text{PMe}_2\text{Ph})_4]$ with HF in MeOH/Et₂O in a borosilicate glass reaction vessel has been reported to give *trans*- $[\text{WF}(\text{NNH}_2)(\text{PMe}_2\text{Ph})_4][\text{BF}_4]$.¹⁴ Spectroscopic evidence for the presence of the tetrafluoroborate anion in $[\text{Cp}^*_2\text{TaF}_2][\text{BF}_4]$ is provided by ¹⁹F NMR and IR spectroscopy. For example, the ¹⁹F NMR signals at δ 21.2 and -154.6 ppm may be assigned to the $[\text{TaF}_2]$ and the $[\text{BF}_4]$ moieties, respectively, while the absorption at 1052 cm^{-1} in the IR spectrum may be attributed to $\nu(\text{B-F})$. The molecular structure of $[\text{Cp}^*_2\text{TaF}_2][\text{BF}_4]$ has also been determined by X-ray diffraction, as illustrated in Figure 2. Selected bond lengths and

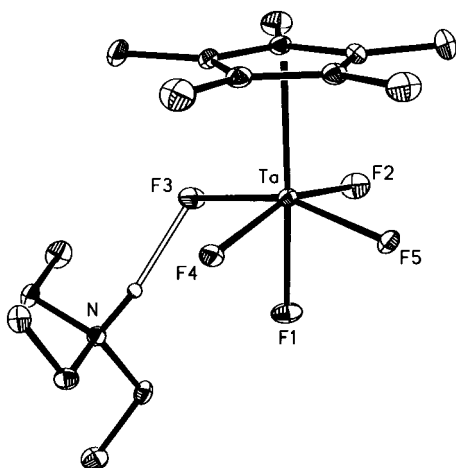
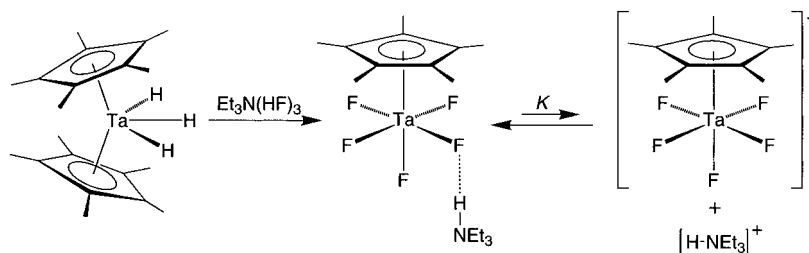
(11) Cationic 16-electron Ta(V) complexes of the type $\{[\text{Cp}^R]_2\text{TaX}_2\}^+$ have also been reported. See ref 9.

(12) McClinton, M. A. *Aldrichim. Acta* **1995**, *28*, 31–35.

(13) The reaction may possibly proceed via initial generation of BF_3 , followed by fluoride abstraction from $\text{Cp}^*_2\text{TaF}_3$.

(14) Chatt, J.; Pearman, A. J.; Richards, R. L. *J. Chem. Soc., Dalton Trans.* **1978**, 1766–1776.

Scheme 3

Figure 4. Molecular structure of $[\text{Et}_3\text{NH}][\text{Cp}^*\text{TaF}_5]$.Table 4. Selected Bond Lengths (Å) and Angles (deg) for $[\text{Et}_3\text{NH}][\text{Cp}^*\text{TaF}_5]$

Ta–F(1)	1.960(2)	Ta–F(2)	1.933(2)
Ta–F(3)	1.970(2)	Ta–F(4)	1.941(2)
Ta–F(5)	1.931(2)	Ta–C(11)	2.527(3)
Ta–C(12)	2.468(3)	Ta–C(13)	2.450(3)
Ta–C(14)	2.491(3)	Ta–C(15)	2.544(3)
Ta–C(24)	2.443(17)	Ta–C(25)	2.421(19)
N–H(1a)	0.98(5)	F(3)⋯H(1a)	1.792(52)
F(3)⋯N	2.766(3)	N–C(31)	1.511(4)
N–C(41)	1.506(4)	N–C(51)	1.504(4)
F(1)–Ta–F(2)	79.98(10)	F(1)–Ta–F(3)	77.94(9)
F(1)–Ta–F(4)	78.82(9)	F(1)–Ta–F(5)	81.05(9)
F(2)–Ta–F(3)	88.52(10)	F(2)–Ta–F(4)	158.80(10)
F(2)–Ta–F(5)	88.58(9)	F(3)–Ta–F(4)	87.10(9)
F(3)–Ta–F(5)	158.98(9)	F(4)–Ta–F(5)	88.12(9)

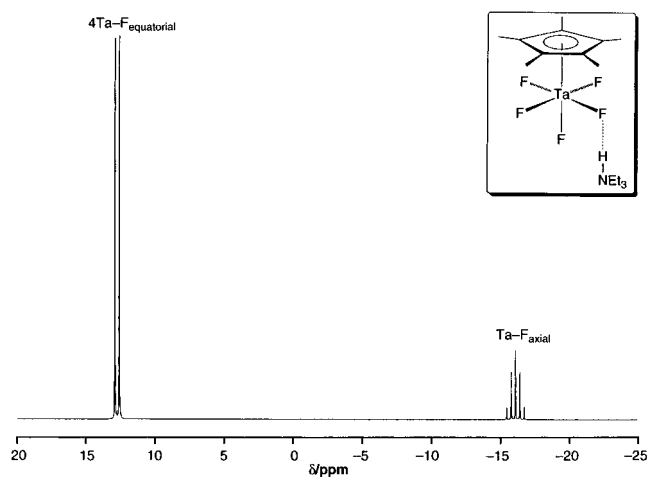
angles are summarized in Table 2, and the average Ta–F bond length of 1.90(4) Å is comparable to the Ta–F bond lengths in other tantalum fluoride complexes. For example the mean terminal Ta–F bond length of complexes listed in the Cambridge Structural Database¹⁵ is 1.905 Å.¹⁶ The related niobium complex $[\eta\text{-C}_5\text{Me}_4\text{Et}_2\text{NbF}_2][\text{PF}_6]$ has been prepared by reduction of $(\eta\text{-C}_5\text{Me}_4\text{Et}_2)\text{NbCl}_2$ with Na(Hg), followed by reaction with $\text{H}[\text{PF}_6]$;¹⁷ for comparison, the average Nb–F bond length is 1.91(1) Å, while the F–Nb–F bond angle is 102.3(4)°.

The fluoro complexes $\text{Cp}^*_2\text{TaF}_3$ and $[\text{Cp}^*_2\text{TaF}_2]\text{[BF}_4]$ are readily interconverted. Thus, treatment of $\text{Cp}^*_2\text{TaF}_3$ with either $\text{Et}_2\text{O}\cdot\text{BF}_3$ or LiBF_4 yields $[\text{Cp}^*_2\text{TaF}_2][\text{BF}_4]$, while reaction of the latter complex

(15) CSD Version 5.14. *3D Search and Research Using the Cambridge Structural Database*; Allen, F. H.; Kennard, O. *Chem. Des. Automation News* **1993**, 8 (1), pp 1, 31–37.

(16) The range of bond lengths is 1.807–2.067 Å.

(17) Brunner, H.; Gehart, G.; Meier, W.; Wachter, J.; Riedel, A.; Elkrami, S.; Mugnier, Y.; Nuber, B. *Organometallics* **1994**, 13, 134–140.

Figure 5. ^{19}F NMR spectrum of $[\text{Et}_3\text{NH}][\text{Cp}^*\text{TaF}_5]$ in benzene (0.08 M).

with excess NaF regenerates $\text{Cp}^*_2\text{TaF}_3$ (Scheme 1). Furthermore, $\text{Cp}^*_2\text{TaF}_3$ is converted to the cyano fluoride complex $\text{Cp}^*_2\text{Ta}(\text{CN})_2\text{F}$ upon reaction with excess Me_3SiCN . The latter fluoro complex is characterized by a ^{19}F NMR spectroscopic signal at $\delta -194.1$ ppm for the $[\text{TaF}]$ moiety. More importantly, the observation of two signals attributable to the $[\text{Ta}(\text{CN})_2]$ group in the ^{13}C NMR spectrum [$\delta 153.0$ (d, $^2J_{\text{C-F}} = 19$ Hz) and 155.7 (d, $^2J_{\text{C-F}} = 21$ Hz)] provides convincing evidence that the fluoride ligand is located in a lateral position.¹⁸

The trihydride complex $\text{Cp}^*_2\text{TaH}_3$ has also proved to be a precursor for other Ta(V) halide complexes. For example, $\text{Cp}^*_2\text{TaH}_3$ reacts sequentially with MeI to give $\text{Cp}^*_2\text{TaH}_2\text{I}$ and $\text{Cp}^*_2\text{TaHI}_2$ (Scheme 2).^{19,20} Similarly, replacement of the hydride ligands is also observed in the reactions of $\text{Cp}^*_2\text{TaH}_3$ with either HCl, CHCl_3 , or CCl_4 , giving $\text{Cp}^*_2\text{TaH}_2\text{Cl}$ ²¹ and $\text{Cp}^*_2\text{TaHCl}_2$ (Scheme 2).²² Each of the complexes $\text{Cp}^*_2\text{TaH}_2\text{X}$ and $\text{Cp}^*_2\text{TaHX}_2$ (X = Cl, I) has the possibility of existing as two isomers, which are distinguished by whether the unique ligand

(18) Despite the fact that the central and lateral cyanide ligands are readily differentiated by ^{13}C NMR spectroscopy, only a single $\nu(\text{CN})$ absorption at 2123 cm^{-1} is observed in the IR spectrum, which is within the range observed for other transition metal cyanide complexes (ca. 1950–2250 cm^{-1}).^{18a} Hanusa, T. P.; Burkey, D. J. In *Encyclopedia of Inorganic Chemistry*; King, R. B., Ed.; Wiley: New York, 1994; Vol. 2, pp 943–948.

(19) Furthermore, $\text{Cp}^*_2\text{TaH}_2\text{I}$ is also obtained by reactions of either $\text{Cp}^*_2\text{Ta}(\text{E})\text{H}$ (E = Se, Te), $\text{Cp}^*_2\text{Ta}(\eta^2\text{-Te}_2)\text{H}$, or $\text{Cp}^*_2\text{Ta}(\text{EPh})\text{H}$ (E = S, Se, Te) with MeI. These are better methods of synthesis than from $\text{Cp}^*_2\text{TaH}_3$ since they reduce the possibility of contamination by $\text{Cp}^*_2\text{TaH}_2\text{I}$. (a) Shin, J. H.; Parkin, G. *Organometallics* **1995**, 14, 1104–1106. (b) Shin, J. H.; Parkin, G. Unpublished results.

(20) The formation of $\text{Cp}^*_2\text{TaH}_2\text{I}$ and $\text{Cp}^*_2\text{TaHI}_2$ provides a marked contrast with a related niobium system in which $[\text{Cp}^{\text{TMS}}]_2\text{NbH}_3$ reacts with RX (RX = MeI, EtBr) to give $[\text{Cp}^{\text{TMS}}]_2\text{NbX}$. See: Antiñolo, A.; Fajardo, M.; Jalón, F. A.; López Mardomingo, C.; Otero, A.; Sanz-Bernabé, C. *J. Organomet. Chem.* **1989**, 369, 187–196.

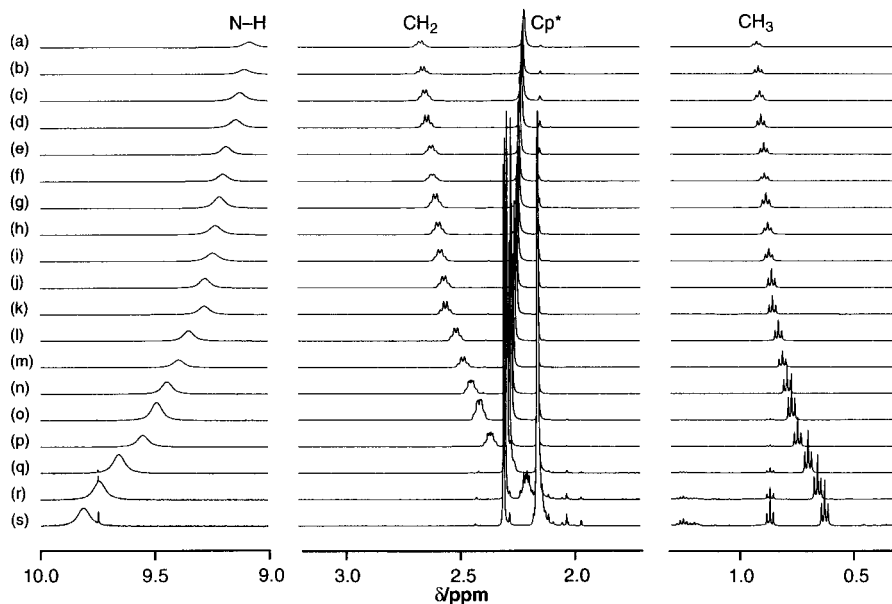


Figure 6. Concentration dependence of the ^1H NMR spectra of $[\text{Et}_3\text{NH}][\text{Cp}^*\text{TaF}_5]$. Initial concentration of $[\text{Et}_3\text{NH}][\text{Cp}^*\text{TaF}_5]$ (mM): (a) 313.5, (b) 296.8, (c) 273.1, (d) 239.1, (e) 214.0, (f) 158.2, (g) 155.9, (h) 144.8, (i) 121.8, (j) 109.8, (k) 103.3, (l) 66.9, (m) 49.1, (n) 36.9, (o) 27.4, (p) 19.2, (q) 9.4, (r) 4.7, (s) 2.3. The singlet at 2.25 ppm is due to mesitylene as an internal standard, while the multiplets at 0.86 (t) and 1.25 (m) ppm are due to pentane impurities present in very dilute solutions.

(H or X) occupies either the central or lateral location of the bent metallocene framework. In all cases, however, the smaller hydride ligands are observed to occupy the more sterically demanding lateral positions. For example, evidence that suggests that $\text{Cp}^*_2\text{TaH}_2\text{X}$ adopts a symmetric structure in which X is located in the central position is provided by the observation of a single resonance for the hydride ligands in the ^1H NMR spectrum. Furthermore, X-ray diffraction studies on the related complexes $\text{Cp}^*_2\text{TaH}_2(\text{EPh})$ (E = S, Se, Te) confirm a symmetric structure with the chalcogenolate ligand occupying the central site.¹⁹ The hydride ligands of $\text{Cp}^*_2\text{TaHX}_2$ (X = Cl, I) also occupy a lateral position, thereby resulting in an asymmetric structure.²³ The molecular structure of the chloride complex $\text{Cp}^*_2\text{TaHCl}_2$ has been determined by X-ray diffraction (Figure 3 and Table 3), but the hydride ligand is disordered as a consequence of the molecule residing on a crystallographic 2-fold axis. Nevertheless, clear evidence that the hydride ligand is located in a lateral position is provided by the observation that the Cl–Ta–Cl bond angle of $76.4(4)^\circ$ for $\text{Cp}^*_2\text{TaHCl}_2$ is significantly smaller than that of $83.3(1)^\circ$ in $\text{Cp}^*_2\text{TaCl}_2$.^{19b}

It is important to emphasize that the use of the $[(\text{C}_5\text{H}_5\text{N})(\text{HF})_4]$ reagent is critical for the syntheses of $\text{Cp}^*_2\text{TaF}_3$ and $[\text{Cp}^*_2\text{TaF}_2][\text{BF}_4]$. Thus, the alternative fluorinating reagent $[\text{Et}_3\text{N}(\text{HF})_3]$ ¹² does not yield either $\text{Cp}^*_2\text{TaF}_3$ or $[\text{Cp}^*_2\text{TaF}_2][\text{BF}_4]$. Specifically, the reaction of $[\text{Et}_3\text{N}(\text{HF})_3]$ with $\text{Cp}^*_2\text{TaH}_3$ results in cleavage of one of the pentamethylcyclopentadienyl ligands to yield $[\text{Et}_3\text{NH}][\text{Cp}^*\text{TaF}_5]$ (Scheme 3). The molecular structure of $[\text{Et}_3\text{NH}][\text{Cp}^*\text{TaF}_5]$ has been determined by X-ray diffraction, as illustrated in Figure 4, with selected bond lengths and angles listed in Table 4. Viewing the Cp^* ligand as occupying a single site, the structure of $[\text{Cp}^*\text{TaF}_5]^-$ may be considered to be based on an octahedron, similar to those of $[\text{Et}_3\text{NH}]_2[\text{OTaF}_5]$ ²⁴ and $[\text{Et}_4\text{N}]_2[\text{F}_5\text{TaOTaF}_5]$.^{25,26} The mean Ta–F bond length

in the latter complex is 1.90 Å, with no significant distinction between the axial and equatorial substituents. ^{19}F NMR studies indicate that the structure of $[\text{Cp}^*\text{TaF}_5]^-$ is static, exhibiting a doublet and quintet at 12.7 and -16.2 ppm, respectively, with a $^2J_{\text{F}-\text{F}}$ coupling constant of 90 Hz (Figure 5). For comparison, $^2J_{\text{F}-\text{F}}$ coupling constants in other $[\text{XTaF}_5]^{n-}$ derivatives are known to be in the range 23–39 Hz.^{25b}

The X-ray diffraction study of $[\text{Et}_3\text{NH}][\text{Cp}^*\text{TaF}_5]$ (Figure 4) demonstrates that the complex exists as an ion pair due to the presence of a N–H \cdots F hydrogen bond. The hydrogen-bonding interaction is close to linear (172°), but is decidedly asymmetric with $d(\text{N}-\text{H}) = 0.98(5)$ Å and $d(\text{F}\cdots\text{H}) = 1.792(52)$ Å.²⁷ Furthermore, the N \cdots F separation of 2.766(3) Å is only 0.18 Å shorter than the sum of their van der Waals radii. These data suggest that the interaction may be classified as a “weak” hydrogen bond.²⁸ Consistent with this suggestion, dissociation of the ion pair is facile in

(21) $\text{Cp}^*_2\text{TaH}_2\text{Cl}$ has not been isolated in pure form, and its characterization is based upon comparison of its ^1H NMR spectrum with that of the iodide analogue, $\text{Cp}^*_2\text{TaH}_2\text{I}$.

(22) $\text{Cp}^*_2\text{TaHCl}_2$ has also been obtained by reactions of either $\text{Cp}^*_2\text{Ta}(\text{Te})\text{H}$ or $\text{Cp}^*_2\text{Ta}(\eta^2\text{-Te})_2\text{H}$ with CCl_4 .^{19b}

(23) The ^1H NMR spectrum of the related *ansa*-complex $[\text{Me}_2\text{Si}(\text{C}_5\text{Me}_4)_2]\text{TaHl}_2$ also indicates an asymmetric structure by virtue of the diastereotopic pairs of methyl substituents on the $[\text{Me}_2\text{Si}(\text{C}_5\text{Me}_4)_2]$ ligand.^{19b}

(24) Furmanova, N. G.; Verin, I. A.; Zanin, I. E.; Zozulin, A. N.; Il'in, E. G. *Kristallografiya* **1991**, *36*, 384–386.

(25) (a) Dewan, J. C.; Edwards, A. J.; Calves, J. Y.; Guerschais, J. E. *J. Chem. Soc., Dalton Trans.* **1977**, 978–980. (b) Sala-Pala, J.; Calves, J. Y.; Guerschais, J. E.; Brownstein, S.; Dewan, J. C.; Edwards, A. J. *Can. J. Chem.* **1978**, *56*, 1545–1548.

(26) The molecular structure of the neutral tungsten analogue, Cp^*WF_5 , has also been determined. Cp^*WF_5 is characterized by doublet and quintet signals at δ 102.2 and 90.8 ppm, with $^2J_{\text{F}-\text{F}} = 140$ Hz. See: Köhler, K.; Herzog, A.; Steiner, A.; Roesky, H. W. *Angew. Chem., Int. Ed. Engl.* **1996**, *35*, 295–297.

(27) $[\text{Et}_3\text{NH}]_2[\text{OTaF}_5]$ also exhibits hydrogen-bonding interactions, but the O and F ligands are disordered. See ref 24.

(28) (a) Emsley, J. *Chem. Soc. Rev.* **1980**, *9*, 91–124. (b) Hibbert, F.; Emsley, J. *Adv. Phys. Org. Chem.* **1990**, *26*, 255–379.

benzene or toluene solution, as evidenced by the highly concentration dependent ^1H NMR spectra of $[\text{Et}_3\text{NH}][\text{Cp}^*\text{TaF}_5]$ shown in Figure 6.²⁹ Analysis of the concentration dependence of the ^1H NMR spectra allows the equilibrium constant for the dissociation (eq 1) to be determined.



At 300 K, the equilibrium constant is $2.3(5) \times 10^{-2}$ M, which corresponds to $\Delta G = 2.25(15)$ kcal mol $^{-1}$. Assuming a value of ca. 15–30 eu for the entropy of dissociation,³⁰ the strength of the hydrogen-bonding interaction may be estimated to be ca. 7–11 kcal mol $^{-1}$,³¹ a range that is consistent with the above classification as a “weak” hydrogen bond.³²

Conclusion

In summary, the trihydride complex Cp^*TaH_3 is a convenient precursor to a series of halide derivatives. Most interestingly, reaction with $(\text{C}_5\text{H}_5\text{N})(\text{HF})_x$ affords the trifluoride Cp^*TaF_3 when carried out in a plastic vessel, but the tetrafluoroborate complex $[\text{Cp}^*\text{TaF}_2][\text{BF}_4]$ when performed in a borosilicate glass vessel. The corresponding reaction of Cp^*TaH_3 with $[\text{Et}_3\text{N}(\text{HF})_3]$, however, results in cleavage of one of the pentamethylcyclopentadienyl ligands to yield $[\text{Et}_3\text{NH}][\text{Cp}^*\text{TaF}_5]$. In the solid state, the latter complex exists as a hydrogen-bonded ion pair, but in solution exists in equilibrium with the dissociated ions.

Experimental Section

General Considerations. All manipulations were performed using a combination of glovebox, high-vacuum, or Schlenk techniques.³³ Solvents were purified and degassed by standard procedures. Cp^*TaH_3 was prepared by the literature method.⁸

^1H NMR spectra were recorded on Bruker Avance 300 DRX, Bruker Avance 400 DRX, and Bruker Avance 500 DMX spectrometers. ^{13}C NMR spectra were recorded on a Varian VXR-300 (75.429 MHz) spectrometer. ^{19}F NMR spectra were recorded on a Bruker Avance 300 DRX spectrometer operating at 282.404 MHz. ^1H and ^{13}C chemical shifts are reported in ppm relative to SiMe_4 ($\delta = 0$) and were referenced internally with respect to the protio solvent impurity ($\delta = 7.15$ for $\text{C}_6\text{D}_5\text{H}$; 7.26 for CHCl_3) or the ^{13}C resonances ($\delta = 128.0$ for C_6D_6 ; 77.0 for CDCl_3), respectively. ^{19}F chemical shifts are reported in ppm relative to CFCl_3 ($\delta = 0$) and were referenced using PhCF_3 ($\delta = -63.72$ ppm) as an external standard.³⁴ All coupling constants are reported in hertz. IR spectra were recorded as

(29) ^{13}C and ^{19}F NMR spectra are also concentration dependent.

(30) For entropies of hydrogen-bonding interactions, see: (a) Arnett, E. M.; Joris, L.; Mitchell, E.; Murty, T. S. S. R.; Gorrie, T. M.; Schleyer, P. v. R. *J. Am. Chem. Soc.* **1970**, *92*, 2365–2377. (b) Kazarian, S. G.; Hamley, P. A.; Poliakov, M. *J. Chem. Soc., Chem. Commun.* **1992**, 994–997. (c) Jaffé, H. H. *J. Am. Chem. Soc.* **1957**, *79*, 2373–2375.

(31) At 330 K, a ΔS of 20 eu contributes 4.5 kcal mol $^{-1}$ to ΔG , while a ΔS of 30.0 eu contributes 9 kcal mol $^{-1}$ to ΔG .

(32) Strong hydrogen bonds are normally considered to have bond energies greater than 12 kcal mol $^{-1}$. For example, the hydrogen bond energy of $[\text{HF}_2]^-$ is ca. 39 kcal mol $^{-1}$. See ref 28.

(33) (a) McNally, J. P.; Leong, V. S.; Cooper, N. J. In *Experimental Organometallic Chemistry*; Wayda, A. L., Darensbourg, M. Y., Eds.; American Chemical Society: Washington, DC, 1987; Chapter 2, pp 6–23. (b) Burger, B. J.; Bercaw, J. E. In *Experimental Organometallic Chemistry*; Wayda, A. L., Darensbourg, M. Y., Eds.; American Chemical Society: Washington, DC, 1987; Chapter 4, pp 79–98. (c) Shriver, D. F.; Drezdson, M. A. *The Manipulation of Air-Sensitive Compounds*, 2nd ed.; Wiley-Interscience: New York, 1986.

KBr pellets on Perkin-Elmer 1430 or 1600 spectrophotometers and are reported in cm^{-1} . Mass spectra were obtained on a Nermag R10-10 mass spectrometer using chemical ionization (CH_4) techniques. C, H, and N elemental analyses were measured using a Perkin-Elmer 2400 CHN elemental analyzer.

Synthesis of Cp^*TaF_3 . A solution of Cp^*TaH_3 (200 mg, 0.44 mmol) in pentane (15 mL) in a plastic vessel was treated with $(\text{C}_5\text{H}_5\text{N})(\text{HF})_x$ (0.06 mL, 0.29 mmol for $x = 9$), and the mixture was stirred at room temperature for 2 h. After this period, the volatile components were removed in vacuo, and the residue was washed with pentane and dried in vacuo to give Cp^*TaF_3 as a white solid (170 mg, 76%). Anal. Calcd for Cp^*TaF_3 : C, 47.3; H, 5.9. Found: C, 46.7; H, 5.9. IR data (KBr pellet, cm^{-1}): 2964 (s), 2911 (vs), 1497 (s), 1441 (vs), 1377 (vs), 1170 (w), 1070 (m), 1024 (s), 957 (w), 810 (w), 761 (w), 690 (w), 597 (m), 545 (vs), 487 (vs), 461 (m), 403 (w). ^1H NMR (CDCl_3): δ 2.05 [s, $\text{C}_5(\text{CH}_3)_5$]. ^{13}C NMR (CDCl_3): δ 10.6 [q, $^1J_{\text{C-H}} = 128$, $\text{C}_5(\text{CH}_3)_5$], 123.8 [s, $\text{C}_5(\text{CH}_3)_5$]. ^{19}F NMR (CDCl_3): δ -52.6 [d, $^2J_{\text{F-F}} = 153$, 2 TaF_{att}], -42.6 [t, $^2J_{\text{F-F}} = 153$, 1 TaF_{cent}].

Synthesis of $[\text{Cp}^*\text{TaF}_2][\text{BF}_4]$. A solution of Cp^*TaH_3 (200 mg, 0.44 mmol) in toluene (20 mL) in a glass vessel was treated with $(\text{C}_5\text{H}_5\text{N})(\text{HF})_x$ (0.6 mL, 2.91 mmol for $x = 9$) and was stirred at room temperature for 20 min. After this period, the volatile components were removed in vacuo, and the residue was extracted into chloroform and filtered. The volatile components were removed from the filtrate, and the residue was washed with pentane and dried in vacuo to give $[\text{Cp}^*\text{TaF}_2][\text{BF}_4]$ as a pale yellow solid (170 mg, 67%). Anal. Calcd for $[\text{Cp}^*\text{TaF}_2][\text{BF}_4]$: C, 41.7; H, 5.2. Found: C, 41.8; H, 5.4. IR data (KBr pellet, cm^{-1}): 2971 (m), 2920 (m), 1488 (s), 1441 (s), 1389 (s), 1282 (w), 1052 (br. vs) [$\nu(\text{BF}_4)$], 873 (w), 791 (w), 697 (vw), 613 (s), 581 (s), 545 (m), 520 (w), 487 (w), 431 (w). ^1H NMR (CDCl_3): δ 2.25 [s, $\text{C}_5(\text{CH}_3)_5$]. ^{13}C NMR (CDCl_3): δ 10.5 [q, $^1J_{\text{C-H}} = 129$, $\text{C}_5(\text{CH}_3)_5$], 128.9 [s, $\text{C}_5(\text{CH}_3)_5$]. ^{19}F NMR (CDCl_3): δ 21.2 [s, TaF_2], -154.6 [s, BF_4].

Interconversion of Cp^*TaF_3 and $[\text{Cp}^*\text{TaF}_2][\text{BF}_4]$. (a) A mixture of $[\text{Cp}^*\text{TaF}_2][\text{BF}_4]$ (ca. 10 mg) and NaF (ca. 10 mg) in CDCl_3 (1 mL) was heated at 80 °C. The formation of Cp^*TaF_3 was observed by ^1H NMR spectroscopy.

(b) A solution of Cp^*TaF_3 (ca. 10 mg) in CDCl_3 (1 mL) was treated with $\text{Et}_2\text{O}\cdot\text{BF}_3$ (ca. 0.02 mL). The reaction was monitored by ^1H NMR spectroscopy, thereby demonstrating the immediate formation of $[\text{Cp}^*\text{TaF}_2][\text{BF}_4]$.

(c) A solution of Cp^*TaF_3 (ca. 10 mg) in CDCl_3 (1 mL) was treated with $\text{Li}[\text{BF}_4]$ (ca. 10 mg). The reaction was monitored by ^1H NMR spectroscopy, thereby demonstrating the immediate formation of $[\text{Cp}^*\text{TaF}_2][\text{BF}_4]$.

Synthesis of $\text{Cp}^*\text{Ta}(\text{CN})_2\text{F}$. A solution of Cp^*TaF_3 (100 mg, 0.20 mmol) in CHCl_3 (10 mL) was treated with Me_3SiCN (137 mg, 1.38 mmol), and the mixture was stirred at room temperature for 1 h. After this period, the volatile components were removed in vacuo, and the residue was washed with pentane and dried in vacuo to give $\text{Cp}^*\text{Ta}(\text{CN})_2\text{F}$ as a white solid (90 mg, 87%). Anal. Calcd for $\text{Cp}^*\text{Ta}(\text{CN})_2\text{F}$: C, 50.6; H, 5.8; N, 5.4. Found: C, 49.9; H, 5.8; N, 5.2. IR data (KBr pellet, cm^{-1}): 2965 (vs), 2912 (vs), 2123 (m) [$\nu(\text{C}\equiv\text{N})$], 1499 (vs), 1433 (vs), 1379 (vs), 1073 (s), 1026 (vs), 852 (w), 811 (w), 755 (w), 600 (w), 550 (vw), 499 (s), 457 (w), 413 (m). ^1H NMR (CDCl_3): δ 2.16 [s, $\text{C}_5(\text{CH}_3)_5$]. ^{13}C NMR (CDCl_3): δ 11.7 [q, $^1J_{\text{C-H}} = 129$, $\text{C}_5(\text{CH}_3)_5$], 121.5 [s, $\text{C}_5(\text{CH}_3)_5$], 153.0 [d, $^2J_{\text{C-F}} = 19$, TaCN], 155.7 [d, $^2J_{\text{C-F}} = 21$, TaCN]. ^{19}F NMR (CDCl_3): δ -194.1 [s, TaF].

(34) Evans, B. J.; Doi, J. T.; Musker, W. K. *J. Org. Chem.* **1990**, *55*, 2337–2344.

(35) For a similar treatment for analyzing equilibrium hydrogen bonding of $(\text{CF}_3)_2\text{CHOH}$ to the hydride ligand of $\text{HW}(\text{CO})_2(\text{NO})(\text{PMe}_3)$, see: Shubina, E. S.; Belkova, N. V.; Krylov, A. N.; Vorontsov, E. V.; Epstein, L. M.; Gusev, D. G.; Niedermann, M.; Berke, H. *J. Am. Chem. Soc.* **1996**, *118*, 1105–1112.

Table 5. Equilibrium Constant Data for Ion Pair Dissociation of [Et₃NH][Cp*TaF₅] at 300 K in Benzene

	NH	CH ₂	CH ₃
<i>K</i> / <i>M</i>	0.028	0.020	0.020
δ ₁ /ppm	8.84	2.82	1.01
δ ₂ /ppm	9.89	2.08	0.58

Synthesis of Cp*₂TaH₂I. MeI (78 mg, 0.55 mmol) was added to a solution of Cp*₂TaH₃ (250 mg, 0.55 mmol) in toluene (20 mL), and the mixture was stirred at room temperature for 1 h. After this period, the volatile components were removed in vacuo and the residue was washed with pentane to give Cp*₂TaH₂I as a pale yellow solid (225 mg, 71%). Anal. Calcd for Cp*₂TaH₂I: C, 41.4; H, 5.6. Found: C, 41.5; H, 5.7. IR data (KBr pellet, cm⁻¹): 2981 (vs), 2957 (vs), 2895 (vs), 2722 (m), 2613 (w), 2533 (w), 2451 (w), 1786 (vs) [ν(Ta–H)], 1487 (vs), 1452 (vs), 1427 (vs), 1375 (vs), 1164 (w), 1069 (w), 1026 (vs), 958 (w), 940 (w), 854 (vw), 804 (w), 727 (m), 599 (w), 551 (vw), 416 (w). ¹H NMR (C₆D₆): δ 1.96 [s, C₅(CH₃)₅], 3.90 [s, TaH₂]. ¹³C NMR (C₆D₆): δ 12.7 [q, ¹J_{C–H} = 127, C₅(CH₃)₅], 107.4 [s, C₅(CH₃)₅].

Formation of Cp*₂TaHI₂. A solution of Cp*₂TaH₃ (ca. 10 mg) in C₆D₆ (1 mL) was treated with MeI (ca. 0.02 mL) and the reaction was monitored by ¹H NMR spectroscopy, which demonstrated that a mixture of Cp*₂TaH₂I¹⁹ and Cp*₂TaHI₂¹⁹ was obtained after a period of ca. 1 h at room temperature.

Synthesis of Cp*₂TaHCl₂. A stirred solution of Cp*₂TaH₃ (200 mg, 0.44 mmol) in pentane (15 mL) was treated with HCl (0.85 mL of a 1.0 M solution in Et₂O, 0.85 mmol) giving a precipitate. The mixture was stirred at room temperature for 1 h and filtered, and the residue was washed with pentane and dried in vacuo to give Cp*₂TaHCl₂ as a white solid (190 mg, 85% based on HCl). Anal. Calcd for Cp*₂TaHCl₂: C, 45.9; H, 6.0. Found: C, 45.3; H, 5.8. MS: *m/z* = 521 (M⁺ – 1). IR data: 2961 (s), 2909 (vs), 2370 (m), 2342 (m), 1778 (m) [ν(Ta–H)], 1623 (w), 1544 (w), 1495 (s), 1437 (s), 1377 (vs), 1261 (w), 1073 (m), 1026 (s), 856 (m), 808 (m), 682 (m), 594 (m), 419 (w). ¹H NMR (C₆D₆): δ 1.83 [s, C₅(CH₃)₅], 12.24 [s, TaH]. ¹³C NMR (C₆D₆): δ 12.0 [q, ¹J_{C–H} = 128, C₅(CH₃)₅], 114.6 [s, C₅(CH₃)₅].

Formation of Cp*₂TaH₂Cl and Cp*₂TaHCl₂. A solution of Cp*₂TaH₃ (ca. 10 mg) in C₆D₆ (1 mL) was treated with CCl₄ (ca. 0.02 mL). The reaction was monitored by ¹H NMR spectroscopy, giving sequentially Cp*₂TaH₂Cl and Cp*₂TaHCl₂ at room temperature. CHCl₃ was observed to react similarly. ¹H NMR spectroscopic data for Cp*₂TaH₂Cl (C₆D₆): δ 1.91 [s, C₅(CH₃)₅], 7.09 [s, TaH]. ¹³C NMR spectroscopic data for Cp*₂TaH₂Cl (C₆D₆): δ 11.9 [q, ¹J_{C–H} = 127, C₅(CH₃)₅], 108.8 [s, C₅(CH₃)₅]. Cp*₂TaHCl₂ was identified by comparison with the ¹H NMR spectrum of an authentic sample.

Synthesis of [Et₃NH][Cp*TaF₅]. A solution of Cp*₂TaH₃ (300 mg, 0.66 mmol) in toluene (15 mL) in a glass vessel was treated with a solution of Et₃N(HF)₃ (177 mg, 1.10 mmol) in toluene (3 mL) and was stirred at room temperature for 2 h. After this period, the volatile components were removed in vacuo, and the residue was washed with pentane and dried in vacuo to give [Et₃NH][Cp*TaF₅] as a white solid (290 mg, 86%). Anal. Calcd for [Et₃NH][Cp*TaF₅]: C, 37.4; H, 6.1; N, 2.7. Found: C, 37.3; H, 6.1; N, 2.7. IR data (KBr pellet, cm⁻¹): 3070 (m) [ν(N–H)], 2988 (m), 2922 (s), 2740 (m), 2679 (m), 1476 (m), 1377 (m), 1166 (w), 1069 (w), 1034 (m), 841 (w), 810 (w), 603 (s), 534 (vs), 455 (m). ¹H NMR (C₆D₆, 0.08 M): δ 2.25 [s, C₅(CH₃)₅], δ 0.84 [t, ³J_{H–H} = 7, HN(CH₂CH₃)₃], δ 2.54 [q, ³J_{H–H} = 7, HN(CH₂CH₃)₃], δ 9.31 [br s, HN(CH₂CH₃)₃]. ¹³C NMR (C₆D₆, 0.08 M): δ 8.2 [q, ¹J_{C–H} = 128, N(CH₂CH₃)₃], δ 10.6 [q, ¹J_{C–H} = 127, C₅(CH₃)₅], δ 45.9 [t, ¹J_{C–H} = 142, N(CH₂CH₃)₃], δ 124.2 [s, C₅(CH₃)₅]. ¹⁹F NMR (C₆D₆, 0.08 M): δ 12.7 [d, ²J_{F–F} = 90, 5 Ta–F_{eq}], δ –16.2 [quintet, ²J_{F–F} = 90, 1 Ta–F_{ax}].

Table 6. Crystal, Intensity Collection, and Refinement Data

	[Cp* ₂ TaF ₂][BF ₄]	[Et ₃ NH][Cp*TaF ₅]	Cp* ₂ TaHCl ₂
lattice	monoclinic	triclinic	orthorhombic
formula	C ₂₀ H ₃₀ BF ₆ Ta	C ₁₆ H ₃₁ F ₅ NTa	C ₂₀ H ₃₁ Cl ₂ Ta
fw	576.2	513.7	523.3
space group	<i>P</i> 2 ₁ / <i>c</i> (No. 14)	<i>P</i> 1̄ (No. 2)	<i>F</i> 2 <i>dd</i> (No. 43)
<i>a</i> /Å	8.702(4)	7.7386(4)	8.380(1)
<i>b</i> /Å	9.947(5)	8.5424(4)	18.118(5)
<i>c</i> /Å	25.240(9)	14.5311(7)	26.578(4)
α/deg	90	97.736(1)	90
β/deg	94.01(3)	99.654(1)	90
γ/deg	90	92.141(1)	90
<i>V</i> /Å ³	2167(1)	936.61(8)	4035(1)
<i>Z</i>	4	2	8
radiation (λ, Å)	0.71073	0.71073	0.71073
ρ (calcd), g cm ⁻³	1.767	1.82	1.723
μ(Mo Kα), mm ⁻¹	5.126	5.911	5.711
θ range, deg	3–45	3–55	3–50
no. of data	3806, 2488	4070	943
	[<i>F</i> > 4σ(<i>F</i>)]		
no. of params	254	221	107
<i>R</i>	0.0740 ^a	0.0214 ^b	0.0413 ^b
<i>R</i> _w	0.0822 ^a	0.0549 ^b	0.1065 ^b
GOF	1.81	1.017	1.22

^a *R* = Σ||*F*_o|| – ||*F*_c||/Σ||*F*_o||; *R*_w = Σ*w*^{1/2}(*F*_o – *F*_c)/Σ*w*^{1/2}*F*_o. ^b *R*₁ = Σ||*F*_o|| – ||*F*_c||/Σ||*F*_o|| for [*I* > 2σ(*I*)]; *wR*₂ = [Σ(*w*(*F*_o² – *F*_c²)²)/Σ(*w*(*F*_o²)²)]^{1/2} for [*I* > 2σ(*I*)].

Determination of the Equilibrium Constant for Dissociation of [Et₃NH][Cp*TaF₅] into Ion Pairs. The equilibrium constant for dissociation of [Et₃NH][Cp*TaF₅] into ion pairs (eq 1) in benzene solution was determined by measuring the concentration dependence of the ¹H NMR chemical shifts of the CH₃, CH₂, and NH resonances of the [Et₃NH]⁺ moiety, according to the expression

$$\delta_{\text{obs}} = \delta_1 \left[1 - \frac{(K^2 + 4KC)^{1/2} - K}{2C} \right] + \delta_2 \left[\frac{(K^2 + 4KC)^{1/2} - K}{2C} \right]$$

where δ₁ and δ₂ correspond to the chemical shifts of [Et₃NH][Cp*TaF₅] and [Et₃NH]⁺, respectively, *C* is the total concentration of tantalum species (i.e., the initial concentration of [Et₃NH][Cp*TaF₅]), and *K* is the equilibrium constant. *K*, δ₁, and δ₂ were determined by computer fitting the observed chemical shifts (δ_{obs}) as a function of concentration (*C*). The best fit parameters for the three sets of resonances are listed in Table 5, from which the equilibrium constant is estimated to be 2.3(5) × 10⁻² M.³⁵

X-ray Structure Determinations. Crystal data, data collection, and refinement parameters for [Cp*₂TaF₂][BF₄], [Et₃NH][Cp*TaF₅], and Cp*₂TaHCl₂ are summarized in Table 6. X-ray diffraction data for [Cp*₂TaF₂][BF₄] and Cp*₂TaHCl₂ were collected on a Siemens P4 diffractometer. The unit cells were determined by the automatic indexing of 25 centered reflections and confirmed by examination of the axial photographs. Intensity data were collected using graphite-monochromated Mo Kα X-radiation (λ = 0.710 73 Å). Check reflections were measured every 100 reflections, and the data were scaled accordingly and corrected for Lorentz, polarization, and absorption effects. X-ray diffraction data for [Et₃NH][Cp*TaF₅] were collected on a Bruker P4 diffractometer equipped with a SMART CCD detector. The structures were solved using direct methods and standard difference map techniques and were refined by full-matrix least-squares procedures using SHELXTL.³⁶ Hydrogen atoms on carbon were included in calculated positions. Systematic absences for [Cp*₂TaF₂][BF₄] were consistent uniquely with *P*2₁/*c* (No. 14). Systematic absences for [Et₃NH][Cp*TaF₅] were consis-

(36) Sheldrick, G. M. *SHELXTL*. An Integrated System for Solving, Refining and Displaying Crystal Structures from Diffraction Data; University of Göttingen, Göttingen, Federal Republic of Germany, 1981.

tent with $P1$ (No. 1) and $\bar{P}1$ (No. 2), of which a satisfactory solution was obtained in the centrosymmetric alternative, $P1$ (No. 2). Systematic absences for $\text{Cp}^*\text{TaHCl}_2$ were consistent uniquely with $F2dd$ (No. 43). Refinement of the Flack x parameter (using TWIN and BASF commands) to a value of 0.0(2) established that the correct absolute structure had been selected.

Acknowledgment. We thank the U.S. Department of Energy, Office of Basic Energy Sciences (#DE-FG02-

93ER14339), for support of this research. G.P. is the recipient of a Presidential Faculty Fellowship Award (1992–1997).

Supporting Information Available: Complete tables of crystallographic data and labeled ORTEP drawings for $[\text{Cp}^*\text{TaF}_2][\text{BF}_4]$, $[\text{Et}_3\text{NH}][\text{Cp}^*\text{TaF}_5]$, and $\text{Cp}^*\text{TaHCl}_2$ (25 pages). Ordering information is given on any current masthead page.

OM980549V